

## INDUCED CRYSTALLIZATION PRINCIPLE FOR RAPID 3D PRINTING OF STEEL MELTS

V.B. Oshurko<sup>1,2</sup>, A.M. Mandel<sup>1</sup>, K.G. Solomakho<sup>1</sup>, V.N. Lednev<sup>2</sup>

<sup>1</sup> *Moscow State Technological University “Stankin”,  
1 Vadkovsky, Moscow 127994, Russia*

<sup>2</sup> *Prokhorov General Physics Institute, Russian Academy of Sciences,  
38 Vavilov str., Moscow 119991, Russia*

A solution for the most important problems in 3D printing technology (long print periods, small build volumes and limited material properties) is proposed. The method is based on the fact that the temperature of melt crystallization can be increased by pressure. The required pressure can be created by an Ampere force caused by the electric current in the melt flow. A magnetohydrodynamic (MHD) model (with heat taken into account) has been developed. It was shown that additional heating of the melt by this current can be decreased by an appropriate choice of tunable parameters and by applying an additional magnetic field. Ranges of parameters, where this induced crystallization can take place, are found.

**Introduction.** Traditional methods of 3D printing based on jet-printing principles ([1], [2]) assume that a liquid substrate (melt) is placed on the already cooled surface to provide proper crystallization. Searching for alternative methods of controlling crystallization via external influence is of significant interest now.

In the present paper, a new simple principle of field-induced crystallization (ICF) for rapid liquid printing for metallic melts is proposed. The idea of the proposed method is as follows. Consider a continuous flow of the melt from a tank or a reservoir through an appropriate nozzle. When an electric current is applied to this continuous melt flow (continuous jet), the flow must be compressed by the well-known Ampere force. Obviously, the pressure inside the flow is controlled by the electric current. On the other hand, increasing pressure leads to an increase of the crystallization temperature [3]. If the pressure in the region, where the flow ends, were high enough, the transition through the crystallization point to the solid state would occur in this region. If crystallization takes place, building of an appropriate 2D scanning procedure and the removal excess material result in the creation of a rapid 3D printer for melts.

However, there is a process that obviously can prevent the crystallization in the described process. Indeed, the increase of the electric current (which is necessary to produce high pressure) leads to a strong additional heating of the flow. On the other hand, there are two processes that can cool the flow and, hence, work 'against' the heating by the electric current. First, in the case of melts, the most effective cooling process is the radiative one. Indeed, the energy loss by radiation is proportional to  $\sim T^4$  (where  $T$  is the temperature) and in the case of melts ( $T \approx 10^3$  K) could be rather efficient. This process depends on the radiating area, e.g., on the flow geometry. Another cooling process is the inflow of the 'unheated' melt from the reservoir due to the motion of the melt in the flow. The efficiency of the cooling in this process depends on the flow velocity.

Thus, *a priori* it is not clear whether there is a region of tunable parameters (flow velocity, electric current, melt temperature, nozzle diameter), where the described crystallization can take place. The purpose of the present work is to build

a theoretical model of all these processes to analyze the possibility of controlled crystallization under the described conditions. It will be shown below that after some modification of the procedure (introduction of an additional magnetic field), the proposed method requires realistic values of the tunable parameters.

**1. Methods: MHD model.** Consider a liquid metal flow (jet) along the  $z$ -axis in the downward direction at an initial velocity  $v_0$ . Let the flow be a stationary process, so that  $d\mathbf{v}/dt = 0$ . It means that the usual (stationary) magnetohydrodynamic equation, which is a Navier–Stokes equation with a magnetic term, could be used [4]:

$$(\mathbf{v}\nabla)\mathbf{v} = \nu\Delta\mathbf{v} - \frac{1}{\rho}\nabla p + \mathbf{g} + \frac{1}{\rho}[\mathbf{j}, \mathbf{B}], \quad (1)$$

where  $\mathbf{v}$  is the velocity,  $p$  the pressure,  $\nu$  the viscosity,  $g$  the acceleration of gravity,  $\mathbf{j}$  the current density, and  $\mathbf{B}$  is the magnetic field.

In our case, the magnetic field is not external and is caused by the electric current in the jet. The magnitude of this magnetic field could be easily estimated. Let the electric current density be constant over the cross-section of the jet. Strictly speaking, the electric current density distribution over the cross-section of the jet should be found from an energy minimization condition (see, for example, [4]). However, this could change our estimation only by a constant coefficient  $\sim 1$ . Since  $\mathbf{B} = \mu_0\mu[\mathbf{j}, \mathbf{r}]$ , we can derive for the magnetic field radial distribution ( $r < R$ , where  $R$  is the jet radius)

$$B(r) = \mu\mu_0jr/2, \quad (2)$$

where the current density is

$$j = I_0/\pi R^2(z). \quad (3)$$

Here  $\mu$  is the magnetic permeability of liquid metal,  $\mu_0$  is the magnetic constant,  $I_0$  is the current value. In cylindrical coordinates, the last term in Eq. (1) has only the radial component which reads as

$$-\frac{\mu\mu_0}{\rho}rj^2, \quad (4)$$

which is the Ampere force (divided by the density  $\rho$ ). As expected, the Ampere force acts along the radius and is directed to the axis of the jet ( $r = 0$ ), i.e. in the direction of compression. It is assumed that the jet regime is very close to a laminar one and the diameter of the jet is smaller than its length. Also the angular and radial components of the total flow velocity  $\mathbf{v} = (v_r, v_\phi, v_z)$  are neglected, so that  $v_r \approx 0, v_\phi \approx 0$ , and further we denote  $v_z = v$ .

We do not use the traditional assumption of fluid incompressibility, because rather high pressures could be achieved in our case (100–1000 kbar) if the electric current is high enough. In addition, the assumption of fluid incompressibility  $div(\mathbf{v}) = 0$  would lead to  $dv_z/dz = 0$  or to  $v_z = \text{const}$ . Hence, if the continuity equation  $Q_0 = \rho v(z)S(z)$  is taken into account (where  $Q_0$  is the mass flux, kg/s,  $S(z)$  is the jet cross-section), the incompressibility leads to a constant jet cross-section  $S(z)$  along  $z$ .

As a result, in the cylindrical  $(r, \theta, z)$  coordinates, the equation for pressure dependence on  $r$  is obtained (for  $\mathbf{e}_r$ )

$$\frac{1}{\rho}\frac{\partial p}{\partial r} = -\frac{\mu\mu_0}{\rho}rj^2. \quad (5)$$

The equation for  $\mathbf{e}_z$  yields  $v$

$$v \frac{\partial v}{\partial z} = \nu \frac{\partial^2 v}{\partial z^2} - \frac{1}{\rho} \frac{\partial p}{\partial z} + g. \quad (6)$$

The next approximation is that  $v_z = v$  does not depend on the radius  $r$ . Indeed, this is obviously a good approximation for the free flow in the absence of fixed walls or tube (in case of tube the flow velocity should be zero at the wall). Then, according to Eq. (7), the pressure  $p = p(z)$  in the right-hand side of Eq. (7) should not either depend on the radius, which contradicts Eq. (5) for  $p$ . This contradiction disappears if we assume that both  $p$  and  $v_z$  also weakly depend on  $r$ . Then we could use  $p$  averaged over  $r$  at any given coordinate  $z$ . Integrating Eq. (5) for  $p(z, r)$  yields

$$p(z, r) = -\mu_0 \mu J^2 \frac{r^2}{2} + C_1, \quad (7)$$

where  $C_1$  is the integration constant. Assuming the weak dependence of  $p(r)$ , we should take  $p(z)$  as the average value (on the area element  $2\pi r dr$ ) over the area  $\pi R(z)^2 = S(z)$ . The condition of continuity of the electric current  $J(z)S(z) = I_0$  also has to be taken into account:

$$p(z) = \frac{1}{\pi R^2} \int_0^R p(z, r) 2\pi r dr = \frac{\mu_0 \mu I_0^2}{16\pi S(z)} + C_1, \quad (8)$$

where the integration constant is just the static pressure.

With regard to the continuity of the substance flow  $\rho v_0 S_0 = \rho v(z) S(z)$  (here  $v_0$  and  $S_0$ , respectively, are the initial velocity and the jet section area at  $z = 0$ ), Eq. (8) can be easily solved. However, the exact solution is expressed in terms of the Bessel functions or Airy functions. As a result, expressions for constants are transcendental equations and could be solved only numerically. To obtain simpler qualitative relations between the parameters, we could consider a very simplified problem by substituting the viscosity in Eq. (17) equal to zero.

In this case, Eq. (17) is simply a differential form ( $d/dz$ ) of the well-known Bernoulli equation [5]. It is easy to see that the pressure caused by the magnetic field of the electric current is nothing more than the energy density of the magnetic field, as it must be in the Bernoulli equation. Thus, our model has the same applicability as the Bernoulli equation. Hence, this equation, modified with respect to the magnetic field, could be written as

$$\rho v^2(z)/2 + \rho g z + P_0 + p(z) = \text{const}, \quad (9)$$

where  $p(z)$  is the pressure caused by the magnetic field and actually equal to the energy density of the magnetic field in the cross-section at the coordinate  $z$ , respectively.

Now we have to define the controlled (e.g., tunable in experiment) parameters of this model. Obviously, the following parameters can be changed in experiment: the total electric current  $I_0$ , the initial section of the jet, i.e. the cross-section area of the nozzle  $S_0$ , the length of the jet  $L$ , and the pressure  $P_0$ . It is easy to see that the pressure  $P_0$  defines the initial velocity  $v_0$ . Further, we can consider the velocity  $v_0$  as a tunable parameter.

First of all, we need to find the pressure  $P_1$  at the end of the jet as a function of these tunable parameters. Let us substitute the cross-section at the end of the

jet  $S_1$  (i.e. at a given distance  $L$ ) into Eq. (8). For this purpose, the Bernoulli equation (9) can be written as

$$\frac{1}{2}\rho v_0^2 + \rho gL + \frac{\mu_0\mu I_0^2}{16\pi S_0} = \frac{\rho v_0^2 S_0^2}{2S_1^2} + \frac{\mu_0\mu I_0^2}{16\pi S_1}, \quad (10)$$

where the left-hand side refers to the upper point of the jet, and the right-hand side to the lower point; we have replaced  $v(L) = v_0 S_0/S_1$  due to the continuity condition. Now it is easy to find the section area  $S_1$  and the corresponding pressure  $P_1$ :

$$S_1 = \frac{S_0 \left( \frac{1}{16\pi}\mu_0\mu I_0^2 + \sqrt{A} \right)}{\left( \rho v_0^2 S_0 + 2\rho gL S_0 + \frac{1}{8\pi}\mu_0\mu I_0^2 \right)}, \quad (11)$$

$$P_1 = \frac{\mu_0\mu I_0^2 \left( \rho v_0^2 S_0 + 2\rho gL S_0 + \frac{1}{8\pi}\mu_0\mu I_0^2 \right)}{16\pi S_0 \left( \frac{1}{16\pi}\mu_0\mu I_0^2 + \sqrt{A} \right)}, \quad (12)$$

where

$$A = (\rho^2 v_0^2 + 2\rho^2 gL) S_0^2 v_0^2 + \left( \frac{1}{8\pi}\rho v_0^2 S_0 + \frac{1}{256\pi^2}\mu_0\mu I_0^2 \right) \mu_0\mu I_0^2. \quad (13)$$

**2. Heat balance.** Since crystallization is the most important process considered here, the temperature distribution in the melt flow is of fundamental importance. Let us consider the temperature regime of the jet of liquid metal exposed to the current. It is clear that this regime is determined by the balance of four heat fluxes. First of all, the melt can cool (lose the energy) due to the radiation into the environment. In case of sufficiently high temperatures (about or higher than the temperature of melting), such losses might not be so small. For this loss of energy (heat transfer) of the jet element with the height  $dz$  and radius  $R(z)$  per unit time we can write (here we neglect the temperature of the medium compared to the melt temperature)

$$dQ_1 = \sigma T^4 \cdot 2\pi R dz, \quad (14)$$

where  $\sigma$  is the Stefan–Boltzmann constant. This heat dissipation is compensated by the heat release due to the electric current:

$$dQ_2 = I_0^2 dz / \chi S(z). \quad (15)$$

There are also two processes that can “equalize” the temperature distribution along the jet. The first one, a convection-like heat flux due to the melt outflow from the reservoir:

$$dQ_3 = \rho C_p \cdot v(z) S(z) dT = \rho C_p \cdot v_0 S_0 dT. \quad (16)$$

We used the continuity equation of matter;  $C_p$  is the specific heat of the metal here. The second one, is the usual heat diffusion due to thermal conductivity:

$$dQ_4 = \kappa \frac{S(z)}{dz} \frac{\Delta T}{dz/L}. \quad (17)$$

As a result, the Fourier equation for the heat balance can be presented as

$$dQ_4 + dQ_3 + dQ_2 - dQ_1 = 0. \quad (18)$$

Let us estimate the contributions of all the components of this equation. The following parameters of steel have been used in the present work:  $T_m = 1790$  K, density  $\rho = 7000$  kg/m<sup>3</sup>, thermal conductivity  $\kappa = 47$  W/(mK), specific heat  $C_p = 825$  J/(kgK), electric conductivity  $\chi = 1.05 \times 10^6$  Ohm<sup>-1</sup>m<sup>-1</sup> [6]. Also, the Stefan–Boltzmann constant is  $\sigma = 5.67 \times 10^{-8}$  W/(m<sup>2</sup>K<sup>4</sup>) and the magnetic permeability of the melt must be about  $\mu \approx 1$  because the melt temperature is always higher than the Curie temperature. Other parameters used in the estimations are:  $I_0 = 1 \dots 1000$  A,  $v_0 = 0.1 - 100$  m/s,  $\Delta T = 1 \dots 100$  K,  $dz = 0.001$  m,  $L = 0.01 \dots 1$  m. It has been assessed that the heat flux due to the thermal conductivity  $Q_4$  is much smaller (several orders of magnitude) than the other components ( $Q_1, Q_2, Q_3$ ) in the wide range of experimental conditions. Thus, it is possible to neglect the contribution of the thermal conductivity with respect to the heating by the electric current and radiation losses. Then the heat balance equation (divided by  $dz$ ) takes the form:

$$\frac{\Delta T}{\Delta z} = \frac{1}{\rho C_p v_0 S_0} \left[ \frac{I_0^2}{\chi S(z)} - 2\pi\sigma R(z)T^4(z) \right]. \quad (19)$$

The equation has no analytical solution, but it could be numerically integrated by substituting the explicit functions  $S(z)$  and  $R(z)$  from the preceding equations. However, our purpose was to analyze the possibility of controlled crystallization in the melt flow, and it is not necessary to search for a solution of this equation.

It should be mentioned that the heat flux  $Q_3$  associated with the melt inflow performs a stabilizing role. If the temperature of the jet is lower than the temperature in the melt reservoir, then the heat flux is positive and heating occurs. In the opposite case, this flow could cool the jet. Since the magnitude of this flux is determined by the initial velocity of liquid, it is possible to control this heat flux by changing the initial velocity  $v_0$ . In other words, increasing the velocity of the jet can compensate excessive heating.

**3. Results and discussion.** The main purpose of our study was to find out whether there was a range of tunable (control) parameters ( $v_0, I_0, S_0, L$ ), where the current-controlled melt crystallization at the end of jet could occur. For this purpose, we had to estimate the pressure value which is necessary for shifting the crystallization temperature up. It is known ([3], [7]) that this shift of the crystallization temperature can take place at rather high pressures, of the order of hundreds of kbar. For steel, the empirical dependence of the melting point on the pressure could be expressed as ([7])

$$T_{cr} = T_m + \alpha \cdot p, \quad (20)$$

where  $T_m$  is the melting point under normal conditions; for steel [6]  $T_m = 1796$  K,  $\alpha = 2.4 \cdot 10^{-8}$  Pa/K can be taken. It means that a pressure of about 100 kbar is needed to change the melting point by 1 K.

To be definite, we assumed that we need to increase the crystallization temperature by  $\delta T = 1$  K. This increase can be achieved, according to Eq. (20), at some pressure  $P_{min} = \delta T / \alpha$ . This gives a condition on the pressure  $P_1 > P_{min}$  and it can be transformed to the condition for the current  $I_0 > I_{min}$ . In other words, the crystallization takes place if the current is greater than some  $I_{min}$ . Then  $I_{min}$  is the solution of the equation

$$\delta T / \alpha = P_1 (v_0, I_0 = I_{min}, S_0, L), \quad (21)$$

where  $P_1$  is given by expression (12). The solution of this algebraic equation of fourth degree in  $I_0^2$  is trivial, but it is too large to be put here. The result as a function of  $I_{min}(v_0)$  is shown in Figs. 1–4

Another condition follows from the balance of heat fluxes. If the electric current producing this pressure creates a heat flux  $I_0^2 dz / \chi S_1$  greater than the heat loss  $\sigma T^4 2\pi (S_1/\pi)^{1/2} dz$ , that does not obligatory mean the increase in temperature. Indeed, according to the heat balance equation, in this case, the “convective” term (due to the inflow) would lead to a decrease of heating. Then, in order for the heating to be still smaller than the increase in crystallization temperature  $\delta T$ , the necessary requirement is that the initial velocity of the flow in the “convective” term must be greater than some minimum velocity  $v_0 > v_{0 \min}$ . This velocity  $v_{0 \min}$  might be determined by a condition  $\Delta T / \Delta z < \delta T / L$ , from which the expression for the calculation of  $v_0$  can be derived

$$\frac{\delta T}{L} = \frac{1}{\rho C_p v_0 S_1} \left( \frac{I_0^2}{\chi S_1} - 2\sigma T_m^4 \pi \sqrt{\frac{S_1}{\pi}} \right). \quad (22)$$

If we assume that the velocity  $v_0$  is given, the condition  $v_0 > v_{0 \min}$  could be expressed as a condition for the maximum current ( $I_0 < I_{\max}$ ) at which cooling by the inflowing melt is still enough to provide  $\Delta T / \Delta z < \delta T / L$ . Then expression (22) defines the function  $I_{\max}(v_0, S_0, L)$ . The result was obtained simply, but it was also too large to be presented here entirely. The calculation of the current  $I_{\max}$  as a function of the velocity  $v_0$  is also shown in Figs. 1–4.

Now we have two functional dependences to find out if the described crystallization mechanism exists: (i)  $I_{\min}$ , i.e. the minimum electric current at which the pressure is already sufficient to increase the crystallization temperature by  $\delta T$ , and (ii) the current  $I_{\max}$  is the maximum current at which the heating by this current is still compensated by the onflowing of the colder melt. The ranges of the parameters, for which  $I_{\max} > I_{\min}$ , are obviously the required conditions for the implementation of the proposed method.

The results of this calculation for the case of steel melt are illustrated in Fig. 1. As could be seen, there are no conditions, where  $I_{\min} < I_{\max}$ . In other words, it is impossible to compensate the ohmic heating by the current (if the current is sufficient to change the crystallization temperature) due to the flow of cooler melt.

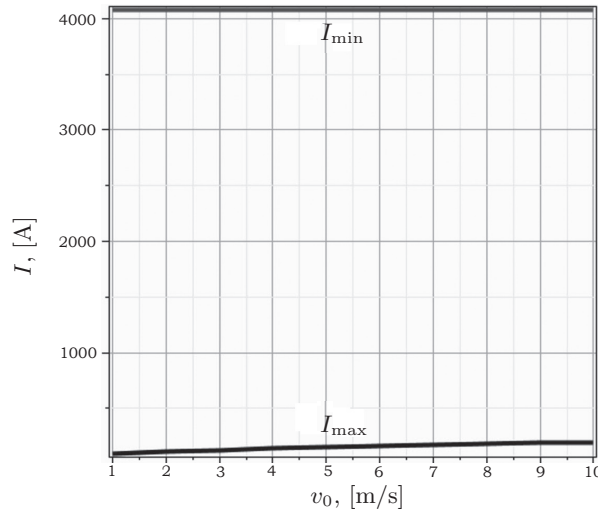


Fig. 1. Region of electric currents  $I$  and flow velocities  $v_0$ , where  $I_{\max} > I_{\min}$  does not exist. Parameters: the jet length is 1.8 cm, the nozzle diameter is 0.35 cm, no external field.

However, it is easy to see that the desired pressure can be reached at a much lower current if an external magnetic field is added. This external field must have the same geometry as the field of the electric current to provide compression of the jet. Hence, the vector  $\mathbf{B}$  must always be directed tangentially to the circle around the axis of the jet. This tangential field could be produced, for example, by a toroidal-shaped solenoid (or a segmented toroidal solenoid, i.e. a toroidal winding with spaces) located around the lower part of the jet. In this case, the additional magnetic field is indeed tangential and it is possible to use for the force  $\mathbf{F} = [\mathbf{j} \times \mathbf{B}]$ . The additional pressure can be expressed as

$$P_{\text{ext}} = \frac{I_0 B}{S_1^2}, \quad (23)$$

where  $S_1$  is the cross-section of the jet at the bottom of the flow.

The purpose of our study was to understand the possibility of realizing the described technique. Therefore, it is possible to ignore the problems of optimal shape of the toroid section, location, and so on. Assume that the described tangential field with an induction  $B$  is created. The functions  $I_{\text{max}}(v_0)$  and  $I_{\text{min}}(v_0)$  at different values of  $B$  are shown in Figs. 2–4. As can be seen in these figures, the results have changed significantly when a relatively small additional field (of only a few tens of millitesla ( $B = 50$  mT)) was applied. As can be seen from Fig. 2, there is a fairly large area with  $I_{\text{max}} > I_{\text{min}}$  with quite realistic values of the tunable parameters: a velocity exceeding 3 m/s and an electric current exceeding 1300 A. Figs. 3–4 show how this region varies with the change in other control parameters, i.e. the jet length  $L$  and the hole diameter  $D$ . It could be seen from Fig. 3 that the increase in jet length up to 5 cm with approximately the same currents requires the increase in initial velocity  $v_0$  to 9.5 m/s.

It is easy to see that the diameter of the nozzle hole is the principal parameter for this method. If the diameter is enlarged to 6.5 mm (Fig. 4), the region, where  $I_{\text{max}} > I_{\text{min}}$  does not exist.

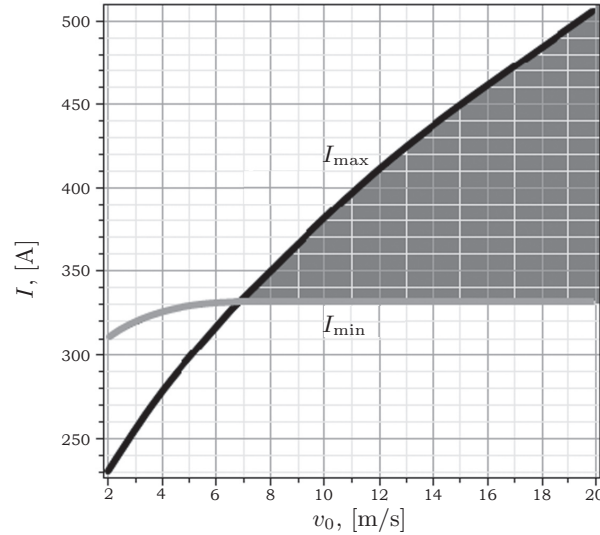


*Fig. 2.* Region of electric currents  $I$  and flow velocities  $v_0$ , where  $I_{\text{max}} > I_{\text{min}}$  exists.  $I_{\text{max}} > I_{\text{min}}$  denotes that the heating by the current can be compensated by a cooler melt inflow and, hence, a field-induced crystallization is possible. Parameters: the jet length is 1.8 cm, the nozzle diameter is 0.35 mm, the external field 50 mT.

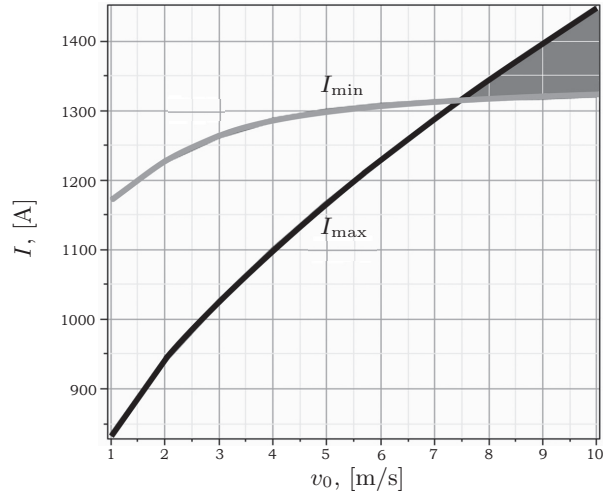


*Fig. 3.* Region of electric currents  $I$  and flow velocities  $v_0$ , where  $I_{\max} > I_{\min}$  exists.  $I_{\max} > I_{\min}$  shows that the heating by the current can be compensated by a cooler melt inflow and, hence, a field-induced crystallization is possible. Parameters: the jet length is 5.0 cm, the nozzle diameter is 0.35 cm, the external field 50 mT.

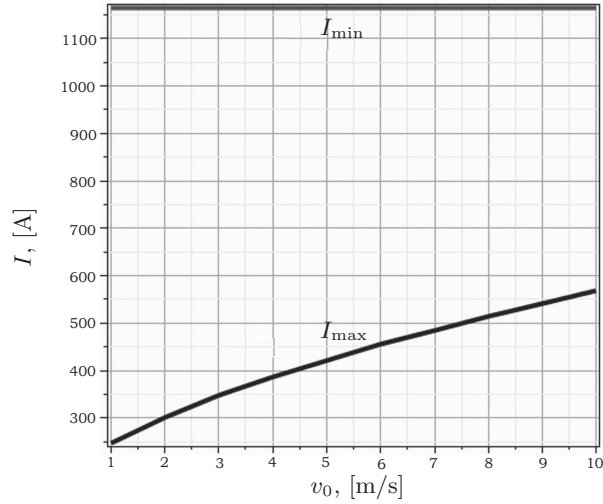


*Fig. 4.* Region of electric currents  $I$  and flow velocities  $v_0$ , where  $I_{\max} > I_{\min}$  does not exist. Parameters: the jet length is 1.8 cm, the nozzle diameter is 0.65 cm, the external field 50 mT.

Thus, there is a wide range of practically real values of parameters at which the described method of 3D printing can be realized.

However, two significant notes to the proposed method should be made. First, we have neglected the viscosity of the melt in the described model. How much could it change the described picture if the viscosity is taken into account? Non-zero viscosity could decrease the initial flow velocity through the hole (there is the so-called “hole ratio” which is determined by the viscosity). However, the lack of velocity due to the melt viscosity can be easily compensated by increasing the pressure  $P_0$  in the original reservoir. Moreover, the viscosity of melts is usually rather small ( $\sim 10^{-7}$  Pa·s). It can be shown that this leads to insignificant changes in velocity along a short path (1.8 cm) of the jet, in our case.



The second note is that the latent heat of crystallization has not been taken into account in our calculations. This additional heat could be released during crystallization and change the picture of the heat balance. However, it is easy to estimate that this heat is much less than the ohmic heating at currents of several thousand amperes. In addition, the small excess of heat could be also always compensated by the choice of  $v_0$  and  $I$  in the experiment within a range of permissible parameters.

**4. Conclusions.** Alternative methods of crystallization controlling via external influence have been proposed. It has been shown that the described method of field-induced crystallization at the end of the melt jet cannot be realized directly because of too much melt heating caused by the electric current. However, it has been found that by adding the external tangential magnetic field the situation can be changed. In this case, there is a wide range of practically real values of parameters, when this method of 3D printing can be realized.

**Acknowledgements.** The work was supported by the Ministry of Education and Science of the Russian Federation (grant No. 9.1195.2017/4.6).

## References

- [1] K. HAJASH, B. SPARRMAN, C. GUBERAN *et al.* Large-scale rapid liquid printing. *3D Printing and Additive Manufacturing*, vol. 4 (2017), no. 3, pp. 123–132.
- [2] T.J. HINTON, Q. JALLERAT, R.N. PALCHESKO. Three-dimensional printing of complex biological structures by freeform reversible embedding of suspended hydrogels. *Science Advances*, vol. 1 (2015), no. 9, pp. 123–132.
- [3] M.M. PANT. Pressure dependence of melting of metals. *Physics of the Earth and Planetary Interiors*, vol. 17 (1978), no. 2, pp. 14–15.
- [4] M.S. TILLACK, N.B. MORLEY. *Magnetohydrodynamics* (McGraw Hill 14th Edition, New York, 1998).
- [5] F.M. WHITE. *Fluid Mechanics, Seventh Edition* (McGraw-Hill, New York, 2011).
- [6] E.R. PARKER. *Materials Data Book for Engineers and Scientists* (McGraw-Hill, New York, 1967).
- [7] H. SCHLOSSER, P. VINET, J. FERRANTE. Pressure dependence of the melting temperature of metals. *Physical Review B – Condensed Matter*, vol. 40 (1989), no. 9, p. 5929.

Received 09.10.2018